Comparison of the damping and stiffness properties of 8wt% yttria stabilized zirconia ceramic coating deposited by the APS and EB-PVD techniques

N. Tassini, K. Lambrinou, I. Mircea, S. Patsias, O. Van der Biest, et al.

N. Tassini, K. Lambrinou, I. Mircea, S. Patsias, O. Van der Biest, R. Stanway, "Comparison of the damping and stiffness properties of 8wt% yttria stabilized zirconia ceramic coating deposited by the APS and EB-PVD techniques," Proc. SPIE 5760, Smart Structures and Materials 2005: Damping and Isolation, (16 May 2005); doi: 10.1117/12.600711

SPIE.

Event: SPIE Smart Structures and Materials + Nondestructive Evaluation and Health Monitoring, 2005, San Diego, California, United States

Comparison of the damping and stiffness properties of 8wt% yttria stabilised zirconia ceramic coating deposited by the APS and EB-PVD techniques

N. Tassini*[a], K. Lambrinou[b], I. Mircea[c], S. Patsias[a], O. Van der Biest[b] and R. Stanway[a]

[a]Dynamics Research Group, Department of Mechanical Engineering, University of Sheffield, Mappin Street, Sheffield S1 3JD, United Kingdom

[b]Department of Metallurgy and Materials Engineering, Katholieke Universiteit Leuven, Kasteelpark Arenberg 44, BE-3001 Heverlee (Leuven), Belgium

[c]Institute of Materials Research, German Aerospace Center (DLR), Linder Höhe, D-51147 Köln, Germany

ABSTRACT

Recent research into the use of thermal barrier coatings has shown that they can provide sufficient additional damping, reducing vibration levels and significantly extending the life of the coated component.

Various deposition techniques may be employed to apply ceramic coatings with Air Plasma Spraying (APS) and Electron Beam - Physical Vapour Deposition (EB-PVD) being the most widely used. However, one has to take into account that even when the starting ceramic material is the same, the microstructures of the resultant coatings depend strongly on the deposition technique.

The objective of this paper is to study of the differences in the damping behaviour and stiffness of an yttria-stabilised zirconia (YSZ with 8%wt yttria) coating deposited by APS and by EB-PVD. Both damping and stiffness of these two YSZ coatings were estimated from tests performed at room and high temperatures. Moreover, this paper presents the microstructural characterisation of these two YSZ coatings using scanning electron microscopy, and attempts a correlation of the differences in their properties to their microstructure.

Keywords: thermal barrier ceramic coatings, YSZ ceramics APS, EB-PVD, damping, stiffness

1. INTRODUCTION

In previous works, thermal barrier ceramic coatings have been shown to provide sufficient damping to be a viable alternative to traditional damping treatments[1-3]. Their damping has also been proven to be virtually unaltered up to temperatures of 600°C, thus being prefarable for high temperature applications to the common polymer-based treatments. Besides, they present a non-linear mechanical behaviour, with stiffness and loss factor dependent on the amplitude of excitation the material undergoes; this aspect requires special characterisation techniques[1,4].

Ceramic coatings can be deposited by different techniques, which, although the starting ceramic material is the same, produce very different microstructures. Prior studies have related the microstructural features of ceramic coatings to their elastic properties[5-6], giving evidence that the microstructure of ceramic coatings can affect deeply their mechanical behaviour.

* n.tassini@sheffield.ac.uk - fax +44 (0) 114 222 7846

Smart Structures and Materials 2005: Damping and Isolation, edited by Kon-Well Wang,
Proceedings of SPIE Vol. 5760 (SPIE, Bellingham, WA, 2005)
0277-786X/05/$15 · doi: 10.1117/12.600711

In this paper focus is placed upon the two most common ceramic coating deposition techniques, Air Plasma Spraying (APS) and Electron Beam - Physical Vapour Deposition (EB-PVD), and the differences in their elastic and damping behaviours are highligthed. Tests were run at the University of Sheffield (USFD), where the Amplitude Dependant Damping (ADD) test rig[1] is capable of running tests over a wide range of strain amplitudes, and at the Katholieke Universiteit Leuven (KUL), where the Impulse Excitation Technique was used to obtain results at lower strains and high temperatures.

Section 2 of this paper briefly describes the two thermal barrier coating deposition techniques studied in this work. Section 3 introduces the characterisation techniques used to obtain results from ceramic coated beams, while Section 4 presents the Finite Element (FE) routine analysis procedure which allows one to obtain the Young's modulus and the loss factor of the material of the coating from the experimental results. The tests results on APS and EB-PVD ceramic coating at room and high temperatures are presented in Section 5 and are subsequently discussed in Section 6. The paper concludes with Section 7, where future work is also discussed.

2. COATING DEPOSITION TECHNIQUES

Ceramic coatings can be applied using various deposition techniques, which may be divided based on their working principle. Different coating deposition techniques generate very different microstructures, although the initial ceramic material might be the same; this results in different mechanical properties of the different coatings. The two major deposition techniques are Plasma Spraying (PS) and Electron Beam - Physical Vapour Deposition (EB-PVD).

PS is a thermal spraying procedure, and consists of injecting the ceramic in powder form into a direct current plasma jet at temperatures up to 10,000K. The mechanism of the coating formation is described in various publications[6-8], and can be carried out in atmospheric conditions (APS) or controlled air or vacuum (VPS).

The typical final shape assumed by the ceramic particles is that of thin lamellae with a "pancake" form, known as "splats". Their "diameters" usually vary between 100 and 200 μm and their thicknesses between 2 and 10 μm[7]. The coating process consists of various passes of the spraying torch over the substrate, forming an overall structure of various layers of splats as shown in Fig. 1.

As shown in Fig. 1, the ceramic coating microstructure is characterised by a complex network of pores associated with imperfect contact between splats[8]. Kroupa et al.[5] have reduced the complexity of the porous spaces present in the microstructure of PS ceramic coatings to four families of defects: larger irregular pores between the splats, small spherical pores inside the splats, "intersplat" cracks between the splats and "intrasplat" microcracks within the splats directed perpendicularly the plane of the splats. Their influence is discussed in Section 6.

In the Electron Beam Physical Vapour Deposition technique the coating's material condenses from the vapour phase onto the desired substrate. The substrate to be coated is heated to temperatures up to 1000 °C. The ceramic material is introduced into the coating chamber as a rod from compacted powder (ingot). The surface of this ingot is melted by a high-power electron beam (EB) and ceramic material is evaporated in the evacuated processing chamber. The vapour uniformly condenses on the surface of the substrate[9], forming a columnar microstructure as shown in Fig. 2.

In order to investigate the differences in the mechanical properties of coatings deposited by these two techniques, a commonly used material for Thermal Barrier Coatings (TBC) was selected, 8%wt Yttria Stabilised Zirconia. The study of its behaviour is one of the topics of the European Union Research and Training Network SICMAC (Structural Integrity of Ceramics Multilayers and Coatings)[10]. Two sets of specimens were coated by APS and EB-PVD and tested respectively at the USFD and KUL, following the procedures described in the following section.

3. TEST PROCEDURE

In the past few years at the USFD a mixed numerical-experimental procedure has been developed for the estimation of the Young's modulus and the loss factor of amplitude dependent materials. This procedure is based on a custom-built test rig, the Amplitude Dependant Damping (ADD) test rig[1], for cantilever type specimens.

In the ADD test rig the specimen is clamped at one end and free to vibrate at the other end, and is excited through the base. Once the excitation force is removed the amplitude of vibration decays at a certain rate and at varying frequency. The decay can be used to obtain the damping value of the coated beam through a numerical analysis[1].

The second testing procedure, namely the impulse excitation technique (IET), is a non-destructive standard test method for the determination of dynamic elastic moduli of materials at ambient temperatures. Data acquisition using the IET equipment available at the KUL is based on digital signal analysis, i.e. the sound of the vibrating specimen is captured by a microphone, digitised, and analysed by the RFDA (Resonance Frequency and Damping Analyser) software (IMCE, Belgium). This program assigns a vibration of the form $x(t) = x_0 e^{-\zeta t} \sin(2\pi f_r t + \phi)$ to a pre-defined number of resonant frequencies f_r. An algorithm simulates the measured signal as a sum of these transient sinusoidal waves, optimising iteratively the parameters x_0, ζ, f_r and ϕ. Having reached an *a priori* convergence criterion, the program gives the final set of resonant frequencies together with a value ζ for every one of them. For each ζ, an internal friction value is calculated according to relation $Q^{-1} = \zeta / (\pi f_r)$ [11-12].

The results obtained from the two test procedures are the resonant frequencies and the damping ratios of the system beam with coating. The value of damping obtained includes the background damping, the damping of the material of the beam and of the coating itself. The background damping can be due to clamping, to losses from fixtures or other rig related factors, as well as the interaction with the surrounding air.

To establish the background damping and its influence on the results, tests are carried out on reference specimens with no coating. The tests are carried out at the same vibration amplitudes and temperatures for both coated and uncoated specimens and the results are used in the following equation, to obtain the added damping due to the coating:

$$Q^{-1}_{added\ damping} = Q^{-1}_{coated\ beam} - Q^{-1}_{uncoated\ beam} \tag{1}$$

where $Q^{-1}_{uncoated\ beam}$ and $Q^{-1}_{coated\ beam}$ are respectively the tests' results from the reference uncoated and the coated specimen. The resulting $Q^{-1}_{added\ damping}$ values obtained are only due to the ceramic coating, and are dependent on its geometry. These damping values are subsequently used together with the resonant frequencies values in a FE routine analysis to estimate Young's modulus and loss factor of the coating, as described in the following section.

4. FINITE ELEMENT ROUTINE

The first step of the FE routine is to create a physical model of the uncoated specimen in Abaqus[13]. The model is run in the first instance with the same boundary conditions as the tests to calculate the resonance frequencies of the uncoated specimen. The following properties of the substrate material are specified: Young's modulus, Poisson's ratio and material density. The results are subsequently compared against the resonant frequencies obtained from experiments.

The model for the coated specimen is created by adding layers on the uncoated specimen model with the software "Fella" developed at USFD[14]. The FE analysis is run again, to estimate the Young's modulus of the coating. An iterative routine gives an initial value for the coating Young's modulus and calculates the corresponding resonant frequencies of interest; the results are compared against the experimental values and modified accordingly. The revised model is run and the whole procedure is repeated until the solution converges to within an error of 0.01%.

Once the Young's modulus of the coating has been established, the damping is calculated using a procedure based on the Modal Strain Energy (MSE) method[2]. The loss factor of the coating is obtained from the following equation

$$\eta_{coating} = \frac{Q^{-1}_{added\ damping}}{MSE\ Ratio} = \frac{U_{coated\ beam}}{U_{coating}} \cdot Q^{-1}_{added\ damping} \tag{2}$$

where $Q^{-1}_{added\ damping}$ is the damping obtained from Eq. 1, and U is the modal strain energy as calculated by the FE analysis for each element set.

This procedure is repeated for every set of test results; in the case of the ADD test rig it gives a set of results at each strain level. Subsequently the results are assembled to give two curves, one for the Young's modulus and one for the loss factor of the coating, as a function of the strain at the substrate-coating interface.

5. RESULTS

The FE procedure described in the previous section has been used to analyse test results from the ADD test rig. Tests were also run on specimens using the IET equipment. However, it was not possible to apply the FE routine to the IET results due to the fact that the coating thickness was not sufficient to cause a significant increase in the beam's natural frequency.

The specimens used for this work are listed in Tab. I together with their configurations and test conditions. The geometry of specimens tested at the USFD is shown in Fig. 3a, while in Fig. 3b is shown the one for specimens tested at KUL.

Reference No.	Coating	Coat. thickness [mm]	Testing procedure	Notes
S1N25	uncoated	-	ADD	High amplitude, RT
S1N11	APS 8YSZ	0.32	ADD	High amplitude, RT
S1N14	APS Bond coat & EB-PVD 8YSZ	0.04 & 0.28	ADD	High amplitude, RT
S3N21	uncoated	-	IET	Low amplitude, HT
S3N18	APS 8YSZ	0.16	IET	Low amplitude, HT

Table I. List of specimens tested.

The position and coverage of the coating's layers in specimens S1N11 and S1N14 correspond to the areas of uniform strain for the first flexural mode (maximum variation of 12.4%) which has been used throughout all the tests with the ADD test rig. This takes into account the strain amplitude dependence of ceramic coatings, so that it is possible to relate their mechanical properties to the strain amplitude. This was not possible for specimen S3N18, where the strain varied by a factor of 5 from the peak value.

All the specimens were manufactured with Inconel® 625 superalloy (In625), a nickel-chromium-molybdenum alloy with low damping (to reduce interference with the damping properties of the ceramic coatings) and high temperature resistance (to allow high temperature tests). As described in Section 2, the material selected for the ceramic coating is 8%wt Yttria Stabilised Zirconia, commonly used for TBCs. Ceramic coating applied by EB-PVD need a metallic bond coat to improve the adhesion of the coating to the substrate: in this work the bond coat material was nickel-cobalt based (NiCoCrAlY), to allow high temperatures tests, and was applied by APS.

The properties of the materials used are given in Tab. II. The values for In625 properties were obtained with the IET technique on an uncoated specimen, while the properties of the bond coat were obtained from the open literature[15]. The density of the 8YSZ coating was obtained by measuring weight and volume of a sample, while the Poissons ratio's value was assumed to be 0.29.

Material	E [GPa]	ν	ρ [kg/dm^3]
In 625	201.67	0.307	8.37
APS Bond coat (NiCoCrAlY**)**	137.9	0.27	7.80
APS 8YSZ	-	0.29	5.00
EB-PVD 8YSZ	-	0.29	5.00

Table II. Properties of materials used.

A FE model was created for each specimen; the models for specimens S1N11 and S3N18 are shown in Fig. 4a and 4b respectively. All the models were run with the same boundary conditions as the tests: clamped-free for the ADD model and free-free for the IET one.

The ADD test procedure and FE analysis have been applied to specimens S1N11 and S1N14 to compare for the first time the damping behaviour of the two most common ceramic coatings, deposited by APS and EB-PVD: the resulting Young's moduli and loss factors from the FE analysis are plotted in Fig. 5a and 5b.

As it is clear from the two plots, both stiffness and damping of the two coatings are amplitude dependant, with the APS coating demonstrating stronger dependence on amplitude. Fig. 5a shows that the EB-PVD coating provides up to 77% higher Young's modulus than the APS coating, while from Fig. 5b it is clear that the APS possesses higher damping (up to five times). These results are discussed in the following section.

Tests with the IET equipment were run from room temperature to 900°C in order to establish the relationship between temperature and damping of APS 8YSZ. Specimens S3N21 and S3N18 were both tested at the first flexural resonant frequency using the same thermal cycle (i.e. heating rate of 5°C/min in vacuum) and amplitude of excitation. The peak amplitude of excitation achieved was less than 5 microstrains.

The added damping as found by applying Eq. 1 due to the APS ceramic coating in specimen S3N18 is plotted in Fig. 6 as a function of temperature. The test results up to a temperature of 600°C are consistent with those discussed previously[3]: the damping provided is nominally constant, with a variation of 18.4%. The damping increases dramatically (more than 80%) up to 900°C. These results are discussed in the following section.

6. DISCUSSION

The tests results on APS and EB-PVD 8YSZ presented in the previous section have highlighted that the coating deposition technique can affect strongly the coating's mechanical properties. The difference in behaviour can be explained by considering their two very different microstructures.

The connection between the structure of PS ceramic coatings and their elastic properties has been the subject of several studies, which provide expressions for the elastic moduli in terms of microstructural parameters. The work by Kroupa et al.[5] mentioned in Section 2 focused on the intersplat and intrasplat cracks: the small elastic openings and partial closing of these microcracks are considered the phenomenon characterising the non-linearity of the PS coating's elasticity.

In a work by McPherson[6], the porosity of PS coatings has been related to their elastic properties: with an increase of the percentage of porosity, the value of the Young's modulus decreases. By observing the columnar microstructure of EB-PVD coatings, it is possible to see that the spaces between columns are small, and thus the porosity is lower than in PS coatings. This can explain the higher values of Young's modulus presented by EB-PVD coatings compared to the APS ones. At the same time the elastic openings and partial closing of the interstices between columns still result in a non-linear elasticity.

Following the results of Kroupa, the authors believe that the damping in PS coating arises from the sliding of the surfaces along the same microcracks responsible for the elastic behaviour[15]. The nature of the load applied to the specimens tested for this work, maximise the sliding along these surfaces. Observing the microstructure of EB-PVD coatings, the size of surfaces which can slide is much lower, thus resulting in a much lower damping of the material, which can be five times lower.

Differences can also be observed in the nature of non-linearity shown by the damping behaviour of the two structures: from Fig. 5b it is possible to observe that in the strain range considered in this work, the non-linearity of APS coatings is stronger than the one of EB-PVD ones; at the same time the damping in PVD coatings seems to keep rising for values of strain above 700 microstrains, suggesting that it might present a behaviour similar to that of APS coatings, shifted at higher strains.

The clear increase in the damping of APS coatings above 600°C might be related to transformation phenomena in the YSZ coating, which occur during the exposure of the TBC to progressively higher temperatures. It has been reported in previous studies[12,17] that the high-temperature transformation of monoclinic to tetragonal zirconia is responsible for an increase in the damping of partially stabilized zirconia ceramics. However, the increase in the damping of the 8YSZ APS coating shown in Fig. 6 has not yet been thoroughly understood.

7. CONCLUSIONS

This paper presents the differences in the mechanical behaviour of ceramic coatings deposited by APS and EB-PVD methods, taking into account their non-linearity. SEM analysis has been employed to relate these differences to the microstructures of the two coatings. The change in damping of APS ceramic coating with temperature has also been taken in consideration.

The results show that EB-PVD coatings possess higher Young's moduli than the APS coating (up to 77% more), while APS has five times higher damping. These properties were related to the microstructural features of the two coatings and to their differences.

Further testing with the IET equipment is planned on specimens with localised APS and EB-PVD coated areas in order to relate the mechanical properties of the two coatings with the strain applied; this way it would also be possible to compare the results found with the IET and the ADD test rig.

Further high temperature IET testing on specimens with thicker APS and PVD coatings is also planned, in order to apply the FE routine and estimate Young's modulus and the loss factor of the two coatings as a function of temperature. High temperature tests are also planned at the University of Sheffield, where the ADD test rig has been provided with a furnace. New specimens are also being prepared to allow tests with the ADD test rig for levels of strain above 800 microstrains.

ACKNOWLEDGMENTS

Work supported in part by the European Community's Human Potential Programme under contract HPRN-CT-2002-00203, [SICMAC][10]. The authors acknowledge the financial support provided through the European Community's Human Potential Programme under contract HPRN-CT-2002-00203, [SICMAC]. The authors are grateful to Plasma & Thermal Coating Ltd, Newport, UK, for preparing all the APS coatings. The authors are also grateful to Mr. David Webster for assistance with the ADD test rig equipment.

REFERENCES

1. S. Patsias, N. Tassini and R. Stanway, "Hard ceramic coatings: an experimental study on a novel damping treatment", *SPIE 11th Annual International Symposium on Smart Structures and Materials*, San Diego, California, 14th-18th March 2004.
2. S. Patsias and R. Williams, "Hard damping coatings: material properties and F.E. prediction method invited paper", *8th National Turbine Engine High Cycle Fatigue (HCF) Conference*, Monterey, California, 14th-16th April 2003.
3. S. Patsias, G. R. Tomlinson and A. M. Jones, "Initial studies into hard coatings for fan blade damping", invited paper, *6th National Turbine Engine High Cycle Fatigue (HCF) Conference,* Jacksonville, Florida, 5th-8th March 2001.
4. S. Patsias, C. Saxton and M. Shipton, "Hard damping coatings: experimental procedure for extraction of damping (internal friction) and modulus of elasticity", Materials Science and Engineering A, **vol. 370 (1-2)**, pp. 412-416, 2004.
5. F. Kroupa and J. Plesek, "Nonlinear elastic behaviour in compression of thermally sprayed materials", Materials Science and Engineering, **vol. A328**, pp. 1-7, 2002.

6. R. McPherson, “A review of microstructure and properties of plasma sprayed ceramic coatings”, Surface and Coatings Technologies, **vol. 39/40**, pp.173-181, 1989.

7. L. Pawlowski, *The Science and Engineering of Thermal Spray Coatings*, John Wiley & Sons Ltd, England, UK, 1995.

8. C. Li, A. Ohomori and R. McPherson, “The relationship between microstructure and Young’s modulus of thermally sprayed ceramic coatings”, Journal of Materials Science, **vol. 32**, pp. 997-1004, 1997.

9. O. Unal, T.E. Mitchell and A.H. Heuer, “Microstructures of Y_2O_3-stabilized ZrO_2 Electron Beam-Physical Vapour Deposition coatings on Ni-base superalloys”, Journal of American Ceramic Society, **vol. 77 (4)**, pp. 984-992, 1994.

10. Internet website, www.sicmac.net

11. G. Roebben, B. Bollen, A. Brebels, J. Van Humbeeck and O. Van der Biest, “Impulse excitation apparatus to measure resonant frequencies, elastic moduli, and internal friction at room and high temperature”, Review of Scientific Instruments, **vol. 68 (12)**, pp. 4511-4515, 1997.

12. G. Roebben, B. Basu, J. Vleugels and O. Van der Biest, “Transformation-induced damping behaviour of Y-TZP zirconia ceramics”, Journal of European Ceramic Society, **vol. 23**, pp. 481-489, 2003.

13. *ABAQUS Standard User’s manual*, version 6.3, Hibbit, Karlsson & Sorensen, Inc., 2002.

14. A. Spencer, Fella - Finite Element Layer Analysis, private comunication, May 2002.

15. G. C. Chang and W. Phucharoen and R. A. Miller, “Finite element thermal stress solutions for thermal barrier coatings”, Surface and Coatings Technology, **vol. 32**, pp. 307-325, 1987.

16. M. Shipton and S. Patsias, “Hard damping coatings: internal friction as the damping mechanism”, *8th National Turbine Engine High Cycle Fatigue (HCF) Conference*, Monterey, California, 14th – 16th April 2003.

17. B. Basu, L. Donzel, J. Van Humbeeck, J. Vleugels, R. Schaler, and O. Van der Biest, “Thermal expansion and damping characteristics of Y-TZP”, Scripta Materialia, **vol. 40**, pp. 759-765, 1999.

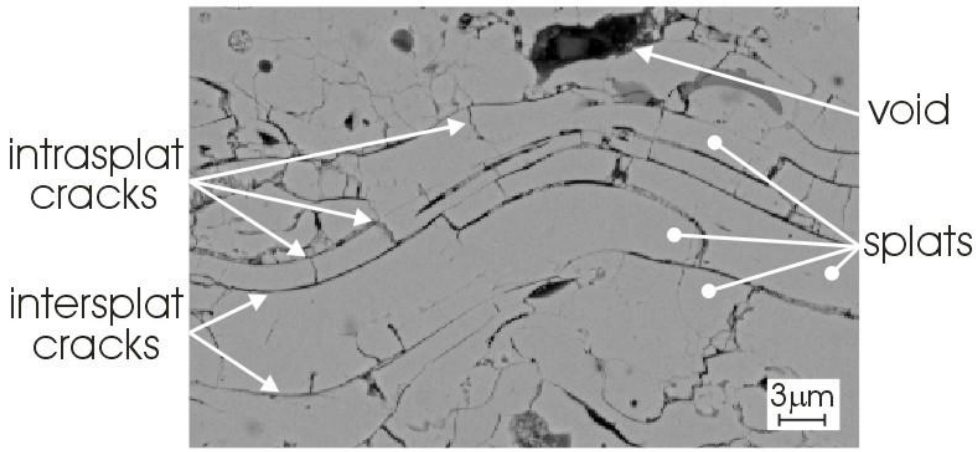

Figure 1. SEM micrograph revealing the cross section of the microstructure of a 8YSZ APS-deposited coating.

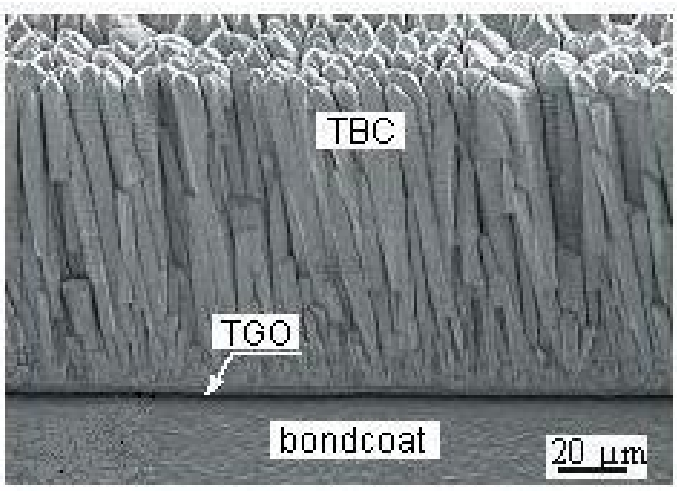

Figure 2. SEM micrograph revealing the cross section of the microstructure of a 8YSZ EB-PVD-deposited coating.

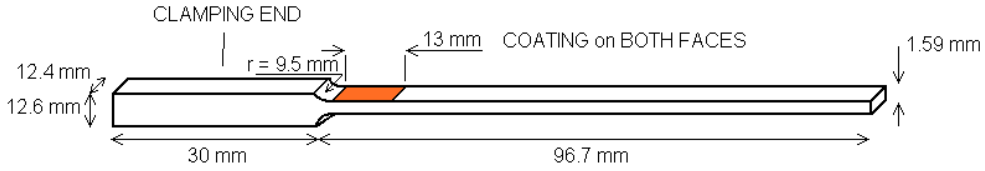

Figure 3a. Geometry of specimen tested with ADD test rig at the University of Sheffield (S1N11 and S1N14).

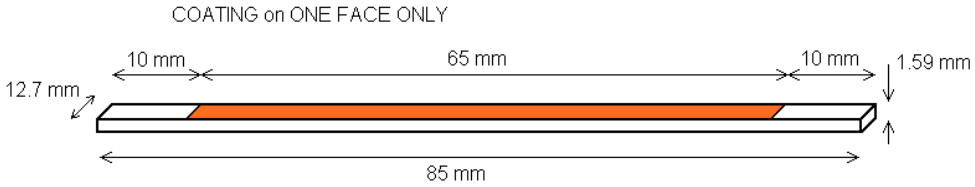

Figure 3b. Geometry of specimen tested with IET at K.U. Leuven (S3N18).

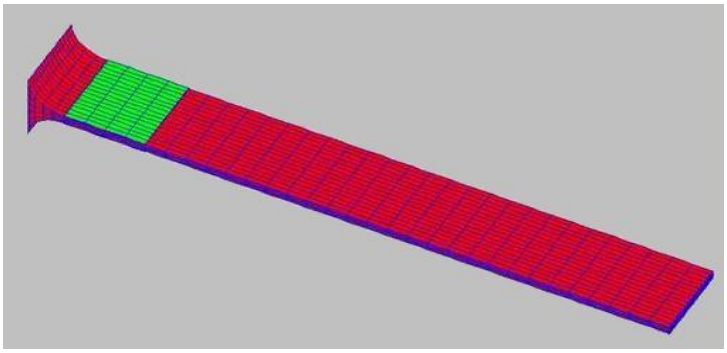

Figure 4a. FE model of specimen S1N11 and S1N14.

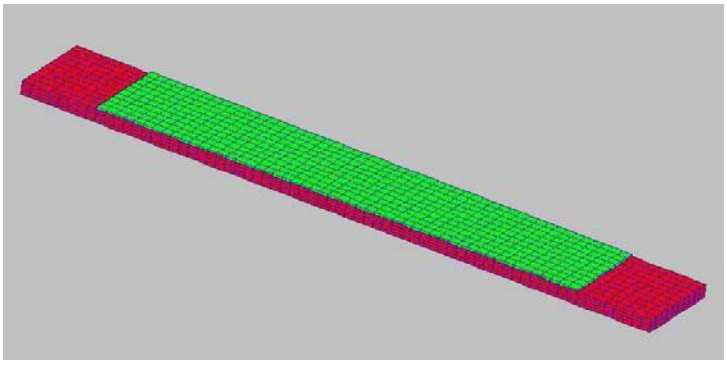

Figure 4b. FE model of specimen S3N18.

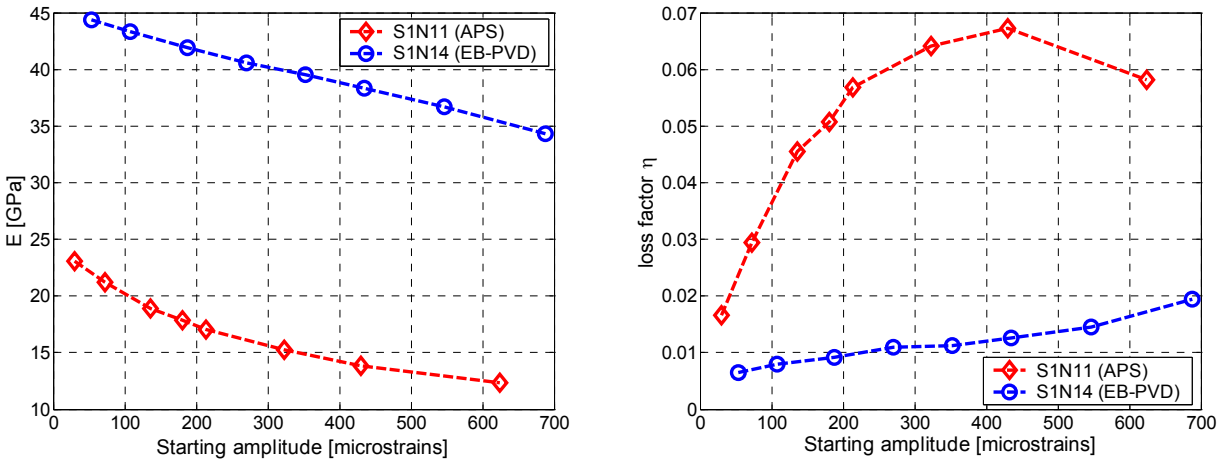

Figure 5. (a) Young's modulus and (b) loss factor of APS and EB-PVD 8YS Zirconia coatings as found with the ADD test rig and FE analysis on specimens S1N11 and S1N14.

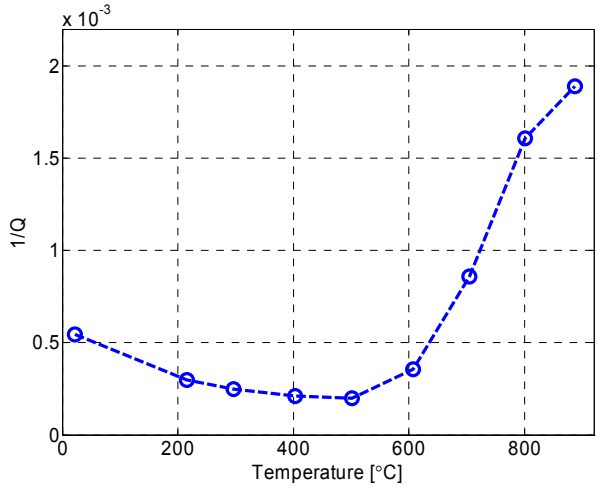

Figure 6. Added damping as a function of temperature due to the APS 8YS Zirconia coating as found with IET equipment on specimen S3N18.